PHYSICAL REVIEW B **97**, 125421 (2018)

Fluid-sensitive nanoscale switching with quantum levitation controlled by α-Sn/β-Sn phase transition

Mathias Boström,[1,2,*] Maofeng Dou,[3,†] Oleksandr I. Malyi,[2,‡] Prachi Parashar,[1,§]
Drew F. Parsons,[4,∥] Iver Brevik,[1,¶] and Clas Persson[2,5,**]
[1] *Department of Energy and Process Engineering, Norwegian University of Science and Technology, NO-7491 Trondheim, Norway*
[2] *Centre for Materials Science and Nanotechnology, University of Oslo, P.O. Box 1048 Blindern, NO-0316 Oslo, Norway*
[3] *Center for Green Research on Energy and Environmental Materials,*
National Institute for Materials Science, Tsukuba, Ibaraki 305-0044, Japan
[4] *School of Engineering and Information Technology, Murdoch University, 90 South Street, Murdoch, Western Australia 6150, Australia*
[5] *Department of Physics, University of Oslo, P.O. Box 1048 Blindern, NO-0316 Oslo, Norway*

(Received 30 May 2017; revised manuscript received 29 November 2017; published 19 March 2018)

We analyze the Lifshitz pressure between silica and tin separated by a liquid mixture of bromobenzene and chlorobenzene. We show that the phase transition from semimetallic α-Sn to metallic β-Sn can switch Lifshitz forces from repulsive to attractive. This effect is caused by the difference in dielectric functions of α-Sn and β-Sn, giving both attractive and repulsive contributions to the total Lifshitz pressure in different frequency regions controlled by the composition of the intervening liquid mixture. In this way, one may be able to produce phase-transition-controlled quantum levitation in a liquid medium.

DOI: 10.1103/PhysRevB.97.125421

I. INTRODUCTION

Nanoelectromechanics have by now developed into quite a mature subject, where one deals routinely with separations between bodies of the order of a few nanometers. For these structures, the Lifshitz forces due to quantum fluctuations [1,2] become accordingly important. This force typically causes attraction between surfaces and thus contributes to stiction, leading to the collapse of devices when surfaces approach each other [3,4]. It has been shown, however, that the Lifshitz force may be repulsive [2] or even in an intricate way change sign as separation increases [5–13]. The development of direct measurements of Lifshitz forces has provided a major thrust in searching viable systems for device engineering [14–17].

Controlled nanomechanical devices could be designed by tailoring the magnitude of the intermolecular interactions between surfaces. Several studies have investigated how this may be achieved through optical excitations and temperature-dependent phase-change materials [18–32]. For example, crystallization of an amorphous Ag-In-Sb-Te film has been predicted to increase the Lifshitz force up to 20% between gold and the alloy surface [28]. However, a phase-transition-controlled sign reversal of the Lifshitz forces is a novel idea that has not, to our knowledge, been proposed yet.

In this paper, we introduce systems in which a phase transition, induced by temperature or other environmental factors, can switch the *sign* of the Lifshitz force between surfaces of a phase-transition material and a thin solid layer across a very thin (<40 Å) liquid film. The model system we have in mind is shown in Fig. 1. We propose using a common phase-transition material, solid tin, which has a phase-transition temperature at $T = 286.5$ K [33,34]. One of its two phases (gray tin; α-Sn) is a semimetal, while its other phase (white tin; β-Sn) is a metal; they have therefore very different dielectric responses. In order to obtain a phase-dependent transition from attractive to repulsive Lifshitz forces, the dielectric functions of the thin solid layer and the intervening liquid must be close and must cross over. One can achieve this requirement by constructing a system with silica (SiO_2) as a thin solid layer and a mixture of two (or more) liquids [10] whose dielectric functions match that of silica. A key element in our proposed model is the influence of the intervening liquid medium between the plates; the effect does not exist if the medium becomes replaced by a vacuum (or air). The transition distance from an attractive to a repulsive Lifshitz force occurs when the attractive and repulsive contributions to the total Lifshitz force from different frequency regions exactly cancel. Thus, the engineering requirements are apparent: the refractive indices of the two pure liquids can lie above and below the refractive index of one of the solid materials. It is then a matter of finding the right combination of the liquid mixture that yields the desired crossover of the dielectric functions of the liquid and the solid. In this work, we choose a particular phase-change material (i.e., tin) just to demonstrate the concept of switching, and we anticipate that this concept can be developed further utilizing other types of metal/nonmetal transitions, for example, by charge injection, chemical insertion, and magnetic phase transition. These systems open up the possibility to make use of the Lifshitz effect as a switch, or actuator, that can be utilized in developments of microelectromechanical (MEMS)

---

[*] mathias.a.bostrom@ntnu.no
[†] maofengdou@gmail.com
[‡] oleksandrmalyi@gmail.com
[§] prachi.parashar@ntnu.no
[∥] d.parsons@murdoch.edu.au
[¶] iver.h.brevik@ntnu.no
[**] clas.persson@fys.uio.no

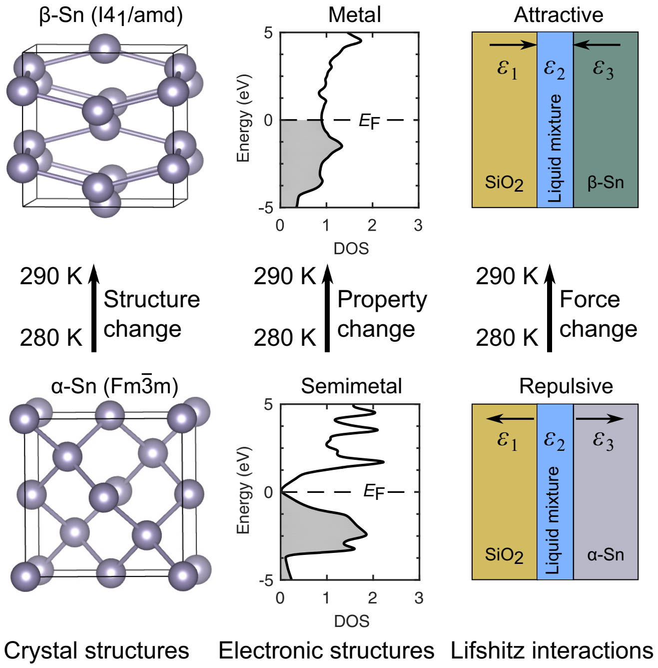

FIG. 1. Scheme of the three-layer system with a switch from repulsive to attractive forces induced by the phase transition from α-Sn to β-Sn. Left: the crystal structures of the two phases. Middle: tin density of states where α-Sn is a semimetal with valence bands fully occupied but β-Sn is a metal with bands partially occupied across the Fermi level E_F. Right: the Lifshitz interactions between SiO_2 and tin surfaces across liquid mixtures at temperatures $T = 280$ and 290 K. ε signifies the dielectric response in each layer.

or nanoelectromechanical (NEMS) systems [3], as well as controlled low-friction nanomechanical devices (Lifshitz repulsion leads to low friction between surfaces [16]).

II. THEORY

Fundamental effects from the Lifshitz force are modeled for the three-layer system as described in Fig. 1. The retarded Lifshitz pressure $p(L)$, between silica and tin surfaces separated across a liquid medium by distance L, is given as a sum over imaginary Matsubara frequencies ($\zeta_n = n 2\pi k_B T/\hbar$) [2],

$$p(L) = \sum_{n=0}^{\infty}{}' (g^{\mathrm{TE}} + g^{\mathrm{TM}}), \tag{1}$$

where the prime on the summation sign indicates that the $n = 0$ term shall be divided by 2. The spectral functions for transverse electric and transverse magnetic modes g^m ($m =$ TE and TM) are

$$g^m = -\frac{k_B T}{2\pi^2} \int d^2k \frac{\gamma_2 r_{21}^m r_{23}^m e^{-2\gamma_2 L}}{1 - r_{21}^m r_{23}^m e^{-2\gamma_2 L}}. \tag{2}$$

Here, r_{ij}^m are the reflection coefficients,

$$r_{ij}^{\mathrm{TM}} = \frac{\varepsilon_j \gamma_i - \varepsilon_i \gamma_j}{\varepsilon_j \gamma_i + \varepsilon_i \gamma_j}, \quad r_{ij}^{\mathrm{TE}} = \frac{\gamma_i - \gamma_j}{\gamma_i + \gamma_j}, \tag{3}$$

where $\gamma_i(i\zeta_n) = \sqrt{k^2 + (\zeta_n/c)^2 \varepsilon_i}$.

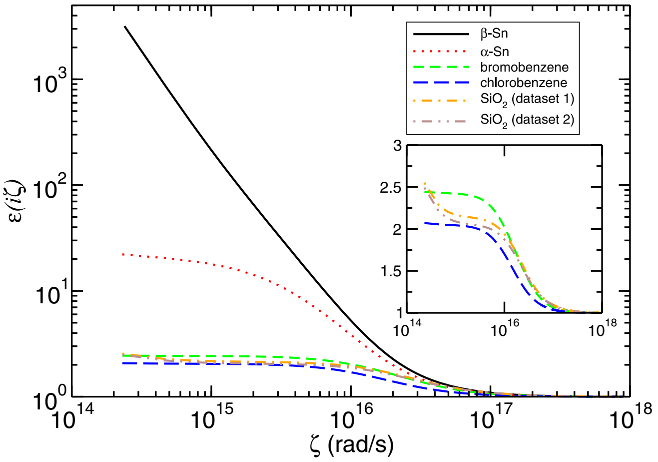

FIG. 2. The dielectric functions of bromobenzene (Bb), chlorobenzene (Cb), and silica (two slightly different data sets) are from van Zwol and Palasantzas [11]. Corresponding spectra for α-Sn and β-Sn are obtained from DFT calculations. The average static dielectric constants are 5.37, 5.75, 4.0, 27.2, and 1.88×10^5, for Bb, Cb, SiO_2, α-Sn, and β-Sn, respectively.

To model the Lifshitz force accurately, detailed knowledge of dielectric functions of all materials involved is essential.

III. MODELING THE DIELECTRIC RESPONSES OF MATERIALS

The primary materials considered in this work are tin (α- and β-Sn) as the phase transition material, silica as the thin solid layer, and a liquid mixture based on bromobenzene (Bb) and chlorobenzene (Cb). In the next section, it will be demonstrated that by mixing liquid Bb with the less polarizable Cb, one obtains the necessary condition for a switch in the Lifshitz pressure from repulsion to attraction when α-Sn undergoes a phase transition to β-Sn.

A. Experimental dielectric functions of silica and liquid mixtures

For the dielectric function of SiO_2 we consider two data sets (i.e., set 1 and set 2) given by van Zwol and Palasantzas [11]; see Fig. 2. Also the dielectric functions of Bb and Cb liquids are also taken from Ref. [11]. The spectrum of SiO_2 lies between those of Bb and Cb (see especially the inset of Fig. 2).

The mixing of two miscible liquids (Cb and Bb here) adjusts the dielectric function of the intervening medium, whereby attractive and repulsive contributions arising from crossings of the dielectric functions of silica and the liquid will occur in different ways for α-Sn and β-Sn (see the remark of Lamoreaux [10] about the possibility to “tune” the mixing such that the force becomes attractive at large separations and repulsive at short range). It is known that in a mixture of Bb and Cb the dielectric constant varies approximately linearly with the relative amount of each of the two components [35]. For the dielectric functions of liquid mixtures, we use the

Lorentz-Lorenz-like model [36] with the susceptibility

$$\chi_2 = \sum_{i=\mathrm{Bb,Cb}} V_i \frac{\varepsilon_{2,i} - 1}{\varepsilon_{2,i} + 2}, \tag{4}$$

where V_i is the volume fraction occupied by the liquid i component that has a dielectric function $\varepsilon_{2,i}$. The dielectric function of the liquid mixture is then given by $\varepsilon_2 = (1 + 2\chi_2)/(1 - \chi_2)$.

Since the calculated transition distances depend on how the dielectric functions are modeled, we have compared the model in Eq. (4) with the volume-average model that assumes a linear dependence of $\varepsilon_{2,i}$ on V_i. The two models describe rather similar dielectric spectra, and they both can give attraction to repulsion transitions. Inaccuracies of describing the exact dielectric responses can thus in an experimental setup be compensated by adjusting the liquid mixture to obtain the switching.

B. Calculated dielectric functions of tin

For the two tin phases we modeled the dielectric functions within the density functional theory (DFT), employing the augmented plane-wave method with local orbitals for Sn d-like orbitals (the APW+lo method) as provided by the WIEN2K package [37]. The imaginary part of the dielectric tensor was calculated from the linear response of the momentum matrix elements describing the transition probability between occupied and unoccupied states [38]. Experimental lattice constants [39] and two-atom primitive cells were used. The regular exchange-correlation potentials with the local-density approximation (LDA) or the generalized gradient approximation (GGA) do not accurately describe tin, especially semimetal α-Sn, due to overestimated hybridization between valence and conduction band states [40]. Instead, we utilize the modified Becke-Johnson meta-GGA exchange potential combined with the LDA correlation potential. With a small k mesh, we have verified a good density of states by comparing with a corresponding hybrid functional calculation. A dense k mesh is, however, needed to describe details in the dielectric response accurately [41]. We therefore calculate it using the regular tetrahedron integration of the irreducible wedge of the Brillouin zone with $58 \times 58 \times 58$ k-mesh grids and an energy grid with a step length of about 0.3 meV. The plane-wave cutoff $K_{\max}$ was determined from $K_{\max} = 8.4/R$ with near touching of the muffin-tin radii $R = 1.404$ Å for α-Sn and 1.511 Å for β-Sn. We have verified that the computed dielectric functions of both the α-Sn and β-Sn phases agree very well with ellipsometric spectra measured in the energy region of 1.2 to 5.6 eV [33]. The corresponding dielectric functions ε_3 as functions of imaginary frequency were obtained from the Kramers-Kronig relation, where the intraband contribution for β-Sn assumed a Drude broadening of 20 meV. The dielectric functions of the two tin phases are displayed in Fig. 2.

IV. RESULTS: FUNDAMENTAL EFFECT

Both tin phases, interacting with silica across pure Bb, experience repulsion at short separation distances. In contrast, across pure Cb, an attractive short-range force is found between both phases of tin and silica. One option to fine-tune the phase-controlled quantum levitation is to use a mixture of liquids tailored experimentally [10]. We show in Fig. 3 the Lifshitz pressure as a function of the distance between silica (data set 1) and tin across three different liquid mixtures: Bb with either 28%, 29%, or 30% Cb added. As expected, the interaction becomes attractive at longer distances as more of the less polarizable Cb is added to Bb. We observe that there is a strong phase-transition dependence in the sign of the Lifshitz pressure. The range of separation distances for the transition from attraction to repulsion depends both on the tin phase and on the specific liquid mixture. It is possible to find the effect for thicker liquid films, but we focus here on liquid mixtures that give a transition from attraction to repulsion in the limit of very thin liquid films. Figure 3 suggests two alternative switching applications: on the one hand, switching in response to a phase transition (e.g., a change in temperature) and, on the other hand, switching in response to a change in liquid composition (i.e., Cb content).

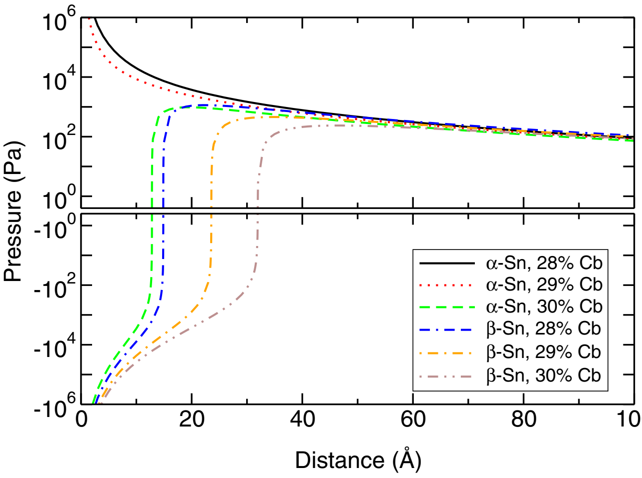

FIG. 3. The Lifshitz pressure as a function of the distance L between silica (data set 1) and α-Sn or β-Sn across a liquid mixture (28%, 29%, and 30% chlorobenzene in bromobenzene), using the dielectric functions from Fig. 2 and mixing according to Eq. (4). Positive values mean repulsion; negative values mean attraction.

We illustrate the relative importance of the $n = 0$ and $n > 0$ contributions to the Lifshitz pressure in Fig. 4. We are facing a situation where the zero-frequency term is as important as it is in systems involving water but not for the reasons anticipated by conventional wisdom (e.g., Ref. [42] or Sec. 6.7 in Ref. [43]). In contrast to liquid water, it is not a high dielectric constant or high dipole moment that drives the dominance of the zero-frequency term in α-Sn. Rather, the dominance is due to a delicate cancellation between negative and positive contributions in the $n > 0$ terms. We have reported this kind of relationship between $n = 0$ and $n > 0$ previously in ice-water systems [44]. Cancellation of $n > 0$ terms leads to repulsion due to the dominance of the zero-frequency term for both Sn phases for liquid films thicker than 50 Å. For thinner liquid films the $n > 0$ terms dominate when tin is metallic, leading to an attraction. The $n = 0$ term dominates when tin is semimetallic, leading to repulsion.

The liquids and mixing ratio need to be chosen and optimized for each system of phase transition considered. That is, with a certain mixture one can obtain repulsion for

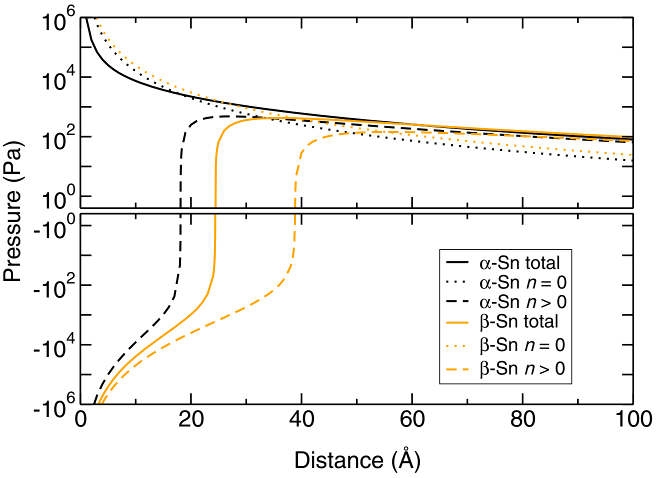

FIG. 4. The total Lifshitz pressure and its contribution from the $n = 0$ term and from $n > 0$ terms in the Matsubara summation. The results are shown for α-Sn and β-Sn as a function of their separation from silica (data set 1) across a liquid mixture (29.1% chlorobenzene in bromobenzene).

both phases, while another mixture yields only attraction. Between these two cases, one can find a range of mixing ratios suitable for a phase-dependent nanoswitch. To exemplify the sensitivity of the levitation with respect to changes in the dielectric functions we present in Fig. 5 the Lifshitz pressures for the two different silica materials (data sets 1 and 2). Each requires a different mixing ratio to work optimally as a phase-controlled nanoswitch. The critical Cb concentration shifts from 29.1% to 76.9%. However, the general behavior is similar after the critical Cb concentration has been tuned to optimize the attraction to repulsion distance. Many different silica materials (and similar materials, like mica or polystyrene) will, when combined with a properly tuned liquid, provide further examples where the phase transition from the semimetallic α-Sn to metallic β-Sn phase changes the short-range Lifshitz interaction from repulsion to attraction. When the same silica material is combined with other liquid mixtures, the sign of the interaction may be independent of the tin phase transition. The reason, of course, is the strict requirement to have a crossing of dielectric functions for the specific silica material and the liquid. When tin turns metallic, the interaction with the second surface turns more attractive (or less repulsive).

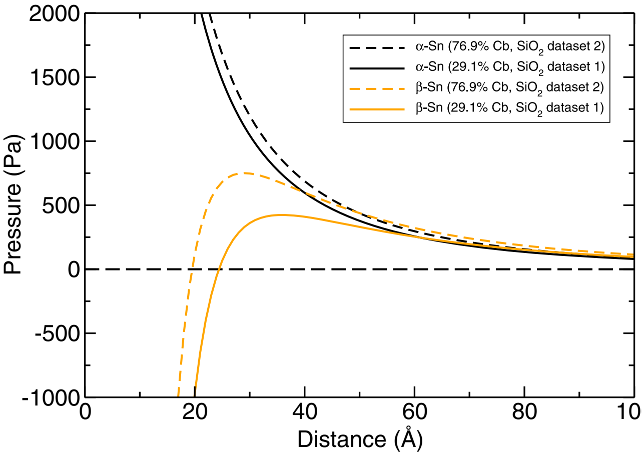

FIG. 5. The Lifshitz pressure as a function of the distance between silica data set 1 and α-Sn or β-Sn across a liquid mixture (29.1% chlorobenzene in bromobenzene). For comparison, we also show the corresponding pressure using an alternative dielectric function for silica data set 2 combined with tin and a different liquid mixture (76.9% chlorobenzene in bromobenzene).

V. RESULTS: FINITE-SIZE SILICA LAYER

While the previous section described the underlying physics of the interlayer interactions for the three-layer system tin/liquid/solid, this section discusses practical aspects in order to detect quantum levitation in the liquid. We investigate the thickness dependences on the solid layer using an extended thickness model [45]. We consider therefore a vertically oriented layer structure, where the solid slab is able to move (or float) up and down in the liquid and the slab feels the buoyancy pressure. This can thus be regarded as a four-layer system of tin/liquid/solid/liquid containing a thin solid layer (typically, SiO_2) with finite thickness d in a liquid (typically, Bb in a mixture with Cb). There is thus a thin film of liquid (thickness L) between the tin and the solid and also liquid above the solid slab. We will not allow the slab to float close to the liquid topmost surfaces, and therefore, the liquid layer can be modeled with a semi-infinite thickness without any major loss in accuracy. Moreover, the bottom tin layer is still considered thick enough to be treated as semi-infinite.

A. Thickness dependence of the Lifshitz pressure

We investigate the thickness dependence of the silica film in the Sn/liquid/SiO_2/liquid system containing a layer of SiO_2 with thickness d in a liquid mixture of 29.1% chlorobenzene in bromobenzene. One can observe in Fig. 6(a) that although the absolute values of the Lifshitz pressures depend on the thickness of SiO_2, the order of magnitudes of the pressure is comparable. The quantum levitation can be observed for all considered thicknesses. Moreover, when the thickness of the SiO_2 layer reaches 1000 Å, the distance dependence of the Lifshitz pressures overlaps in a large range of liquid layer thicknesses with that from the semi-infinite SiO_2 layer in the three-layer model, as shown in Fig. 6(b). Thus, 1000 Å is large enough to be approximated as a macroscopic thickness.

B. Buoyancy pressure

The net buoyancy pressure b on a SiO_2 slab in liquid due to gravity and difference in densities of the SiO_2 film and the surrounding liquid mixture can be estimated using $b = (\rho_{\text{liquid}} - \rho_{\text{silica}})gd$, where g is the gravitational acceleration. With typical values for the densities of the liquid mixture, ρ_{liquid}, and of SiO_2, ρ_{silica}, and a thickness of the SiO_2 slab of $d = 1000$ Å the buoyancy pressure is $b \approx -1.2$ mPa, where the negative sign indicates attraction. This value is negligible compared to the Lifshitz pressure at small separation distances ($L < 20$ Å), where the quantum levitation occurs as shown in Fig. 7(a). Figure 7(b) demonstrates that the attractive buoyancy pressure can compensate the long-range repulsive Lifshitz

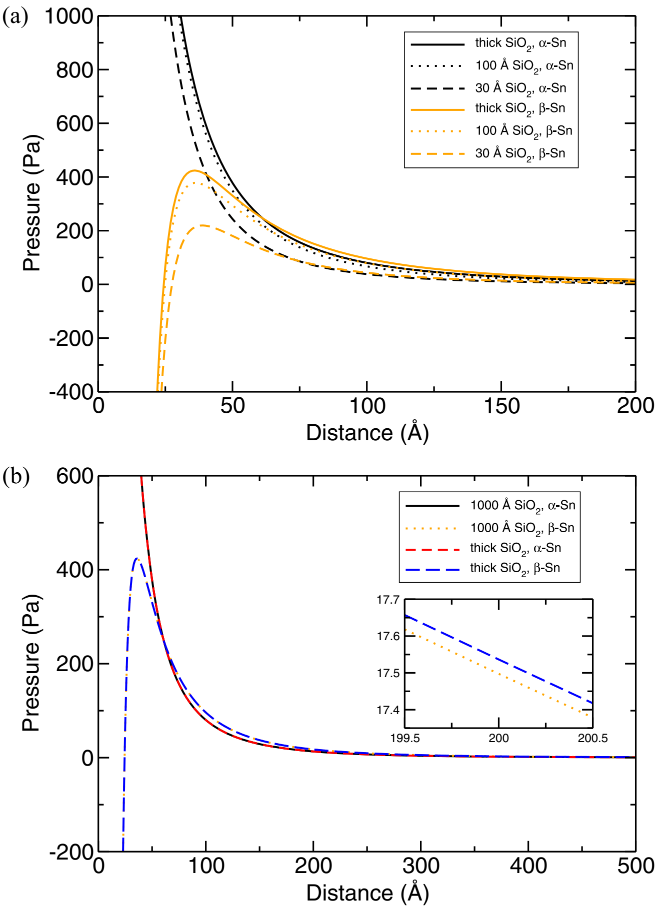

FIG. 6. (a) The Lifshitz pressure as functions of the separation distance L between SiO$_2$ (data set 1) and α-Sn or β-Sn across a liquid mixture (29.1% chlorobenzene in bromobenzene) for the four-layer system with different thicknesses d of the SiO$_2$ layer. Here, "thick" implies the semi-infinite layer of SiO$_2$ used in the three-layer system (Fig. 1). (b) Comparison of the Lifshitz pressures for a 1000-Å-thick SiO$_2$ layer and the semi-infinite layer of SiO$_2$.

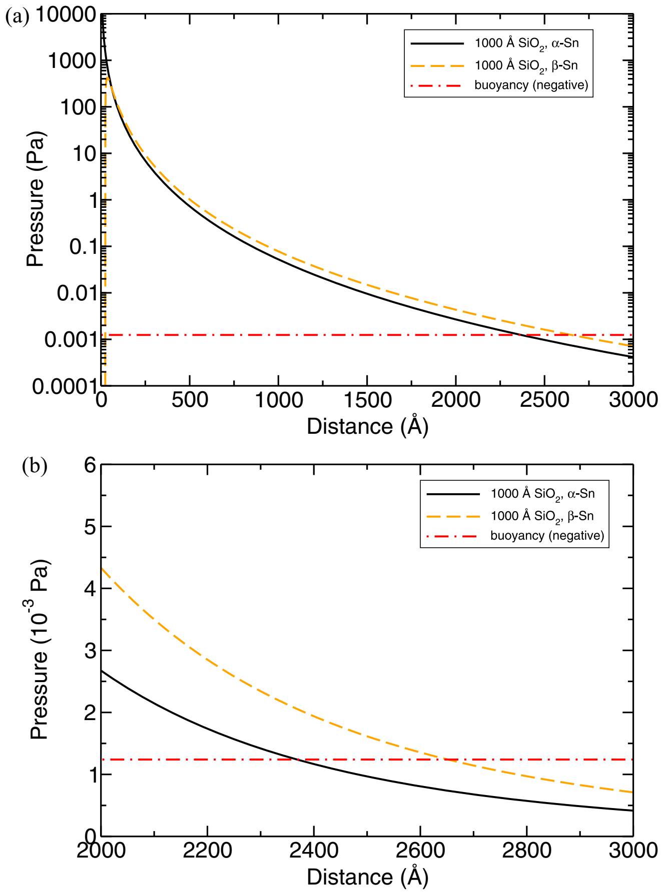

FIG. 7. (a) The Lifshitz pressure as a function of the separation distance between SiO$_2$ (data set 1) and α-Sn or β-Sn across a liquid mixture (29.1% chlorobenzene in bromobenzene) compared to the attractive buoyancy pressure (here, presented on a positive scale). (b) Magnification of the distance region where the repulsive Lifshitz and the attractive buoyancy pressures compensate each other.

contribution at large separations. Intriguingly, α-Sn and β-Sn exhibit a noticeable difference in their respective equilibrium distances, where the net pressure due to the Lifshitz and buoyancy contributions vanishes; they differ by more than 200 Å, which is obvious in Fig. 7(b). However, although the effect is induced by the phase transition, it is not linked directly to the quantum levitation found for the small separation distances.

C. Role of dielectric properties of interacting materials

When the dielectric function for SiO$_2$ (data set 1) is replaced with different parameterizations corresponding to a different SiO$_2$ sample (data set 2), one can observe in Fig. 8(a) that the attraction to repulsion transition disappears. This effect is expected as a noticeable variation in the dielectric properties has been reported in previous works [11,46]. The difference between the two different SiO$_2$ samples (i.e., data set 1 and data set 2) may appear to be small (see Fig. 2), but Fig. 8(b) demonstrates that the spectral functions are very different. With the alternative dielectric function of SiO$_2$ (data set 2), the repulsive contributions to the Lifshitz pressure are enhanced, and the attractive contributions to the Lifshitz pressure are reduced compared to the corresponding results for the SiO$_2$ data set 1. To obtain attraction for the interaction between the silica data set 2 and tin, one must reduce the magnitude of the dielectric function of the liquid. This change can be achieved by increasing the ratio of chlorobenzene in bromobenzene, as described by Fig. 8(c). In the region between the different limits with only repulsion and with only attraction, there is a ratio region where phase-transition-controlled attraction to repulsion transitions can occur. It is worth noticing that the utilization of different models for the dielectric function of the liquid mixture can result in a variation of absolute values of the Lifshitz pressure. Nevertheless, the quantum levitation can still be achieved by making a small change in the liquid ratio, as demonstrated in Fig. 8(d).

Phase-transition-induced attraction to the repulsion of the Lifshitz pressure can also be observed for other systems of materials. In particular, it is found for the interaction of a 1000-Å-thick polystyrene film with an α-Sn or β-Sn slab in a liquid mixture of methanol and bromobenzene [see Figs. 9(a) and 9(b)]. The dielectric functions of polystyrene,

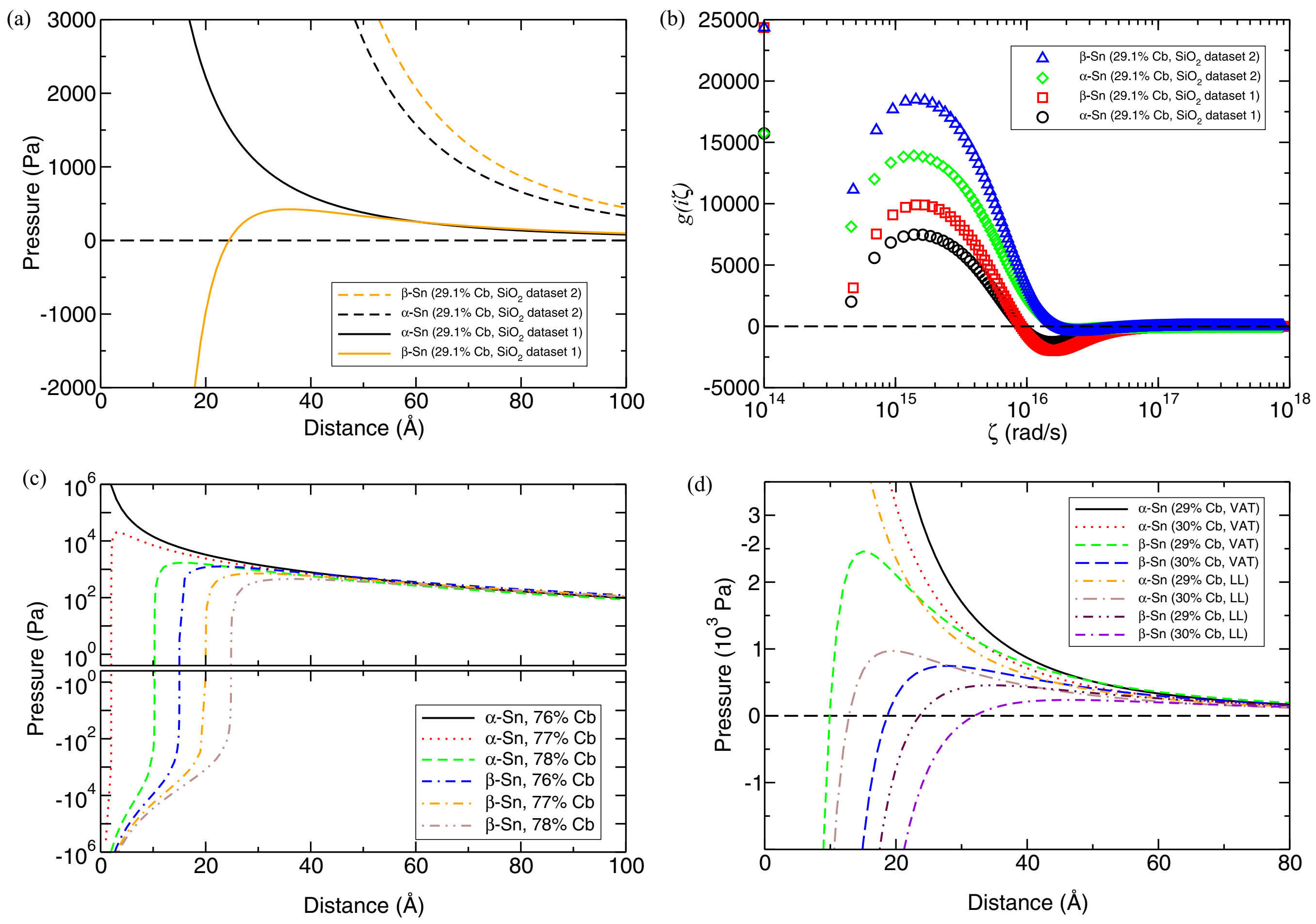

FIG. 8. (a) The Lifshitz pressure as a function of the separation distance between $\mathrm{SiO_2}$ and α-Sn or β-Sn across a liquid mixture of chlorobenzene and bromobenzene using two different parametrizations for the dielectric function of $\mathrm{SiO_2}$, i.e., data sets 1 and 2. (b) Spectral functions revealing the contribution of each frequency mode to the Lifshitz pressures for the two different dielectric functions of $\mathrm{SiO_2}$. The zero-frequency term is divided by a factor of 2. (c) The Lifshitz pressure as a function of the separation distance between $\mathrm{SiO_2}$ and α-Sn or β-Sn across a liquid mixture of chlorobenzene and bromobenzene using $\mathrm{SiO_2}$ data set 2; this can be compared with Fig. 3, where $\mathrm{SiO_2}$ data set 1 is used. (d) The Lifshitz pressure as a function of the separation distance between $\mathrm{SiO_2}$ and α-Sn or β-Sn across a liquid mixture of chlorobenzene and bromobenzene using $\mathrm{SiO_2}$ data set 1 with two different models to describe the dielectric function of the liquid mixture, namely, the Lorentz-Lorenz-like (LL) and the volume-average theory (VAT) models.

methanol, and bromobenzene are also taken from van Zwol and Palasantzas's work [11]. The intervening liquid dielectric function needs to have a crossover with the dielectric function of one of the solid materials to obtain the levitation, but the liquid is a mixture of the two pure liquids whose dielectric functions can lie on either side of the solid [Fig. 9(a)]. Thus, the engineering requirements are obvious: the refractive indices of the two pure liquids can lie above and below the refractive index of one of the solid materials. It is then a matter of finding the right combination of the liquid mixture that yields the desired crossover of the dielectric functions of the liquid mixture and the solid. Hence, it is possible to achieve quantum levitation controlled by the α-Sn/β-Sn phase transition with combinations of different materials. It is noticeable in Fig. 9(b) that there the β-Sn system yields more repulsion than α-Sn. This reversal of behavior occurs due to the difference in frequency regions that give positive and negative contributions to the Lifshitz pressure. Since the zero frequency contributes repulsion, the resulting pressure for both systems is repulsive at distances beyond 760 Å for α-Sn and 470 Å for β-Sn, where the lower-frequency-mode contributions dominate. Thus, there are two crossings of zero pressure, with multiple extreme points, in the pressure curves for the polystyrene-liquid-(β-Sn) system.

D. Thermal fluctuation

We identify two distinct ways in which the system is affected by thermal fluctuations. First, the contribution of the thermal fluctuations to the Lifshitz force is already accounted for [47] through the use of Matsubara frequencies ζ_n in Eq. (1). Second, the proposed system is also subject to classical thermal fluctuations arising from the kinetic energy of the surfaces at temperature T. Kinetic energy of the surface (a type of Brownian motion) causes the distance between surfaces to fluctuate. The stability of the system with respect to classical thermal fluctuations can be established by considering a finite contact area between tin and $\mathrm{SiO_2}$ surfaces. The interaction energy is shown in Fig. 10, evaluated from the pressure

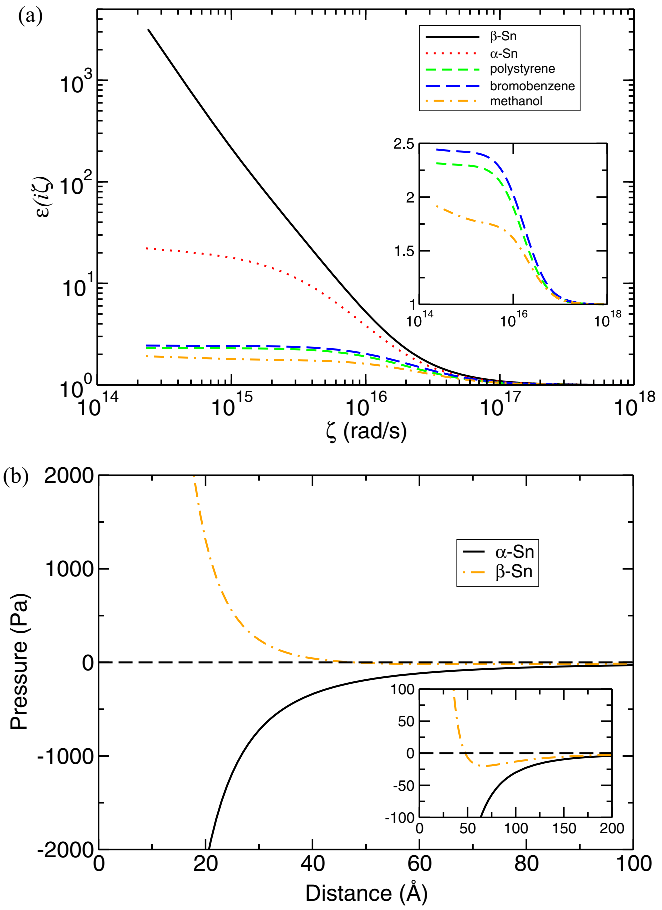

FIG. 9. (a) Dielectric functions of materials used in calculations of (b) the Lifshitz pressure as a function of the separation distance between polystyrene (data set 1) and α-Sn or β-Sn across a liquid mixture of 29% methanol in bromobenzene. The static dielectric constant is 2.45 for polystyrene and 32.9 for methanol; data for the other materials are found in Fig. 2.

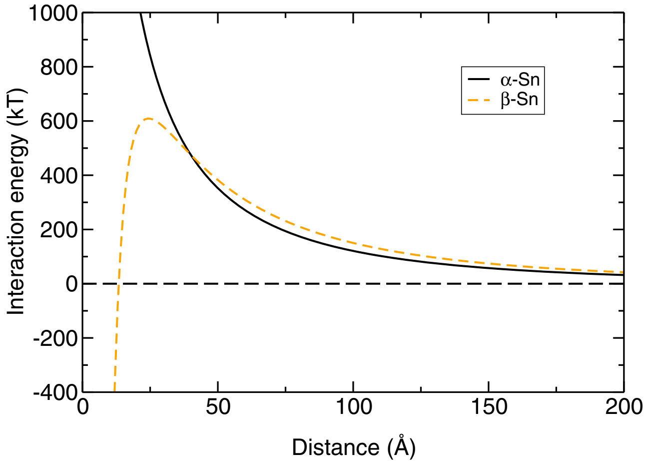

FIG. 10. Interaction energy between SiO_2 (data set 1) and α-Sn or β-Sn across a liquid mixture (29.1% chlorobenzene in bromobenzene) as a function of the distance. The interaction energy is estimated from the pressure by conversion to a $0.1 \times 1 \times 1 \mu m^3$ slab of SiO_2. The temperatures are 280 and 290 K for α-Sn and β-Sn, respectively.

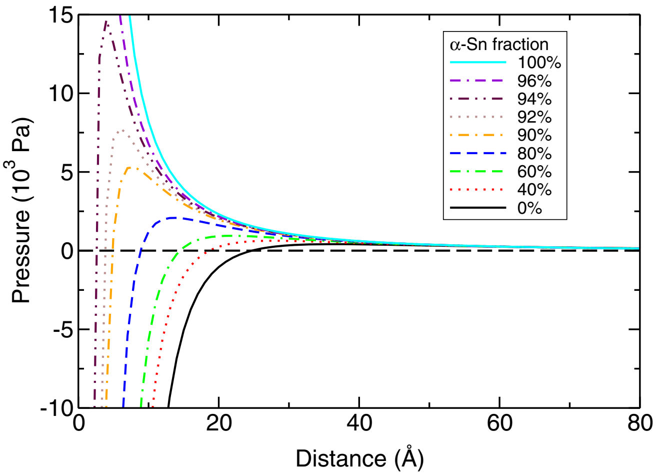

FIG. 11. The Lifshitz pressure as a function of the distance L between silica (data set 1) and an α-Sn/β-Sn mixture across a liquid mixture (29.1% chlorobenzene in bromobenzene) for the three-layer system (Fig. 1). The pressure is given for a partial tin phase transition at $T = 286.5$ K indicated by the fraction of α-Sn coexisting with β-Sn.

assuming a 1000 Å $= 0.1$ μm thick SiO_2 slab with a 1-μm^2 contact area. The thermal kinetic energy is of the order of $k_B T$; thus, as a rule of thumb, an interaction of more than $100 k_B T$ is robust with respect to thermal fluctuations, while an interaction weaker than $10 k_B T$ is reversible (not mechanically stable) [48–50]. The repulsive barrier indicates that the attractive force is stable when the separation between β-Sn and SiO_2 is within $L \approx 20$ Å. At the same length scale, the repulsive interaction found for α-Sn exceeds 600 $k_B T$, indicating stable repulsion.

With these properties the system can be conceived as a trigger switch, initially set up for the β-Sn phase in close contact ($L < 20$ Å) with the SiO_2 slab in the liquid mixture. When a tin phase transition is triggered, α-Sn repulsion pushes the SiO_2 slab outwards. The device will need to be reset when tin is transformed back to the β-Sn phase, overcoming the $600 k_B T$ barrier either mechanically or by flushing with excess chlorobenzene for which the Lifshitz pressure is negative for all separation distances.

VI. DISCUSSION

It is of interest to apply a more comprehensive perspective and ask, will it be practically possible to apply this kind of phase-transition system as an actuator?

The time scale for the complete tin phase transition may be more than 10^4 s [51]. In Fig. 11 we show how the Lifshitz pressure varies during the process of conversion from α- to β-Sn, when the two phases coexist. The dielectric functions of the α-Sn/β-Sn mixture as well as of the liquid were evaluated using the Lorentz-Lorenz-like relation, Eq. (4), and we choose the three-layer system with semi-infinite SiO_2 thickness as described in Fig. 1. The switch in pressure occurs after only 6% conversion, at 94% α-Sn. It follows that the switch from repulsion to attraction can be achieved at a faster time scale than the time required for full conversion.

A second consideration for the practicality of this design of actuator is frictional resistance from the fluid medium. An actuator executing oscillations will necessarily be exposed to viscous drag forces. In order to work properly, the decay time from the drag has to be much shorter than the time needed for the phase transition. In this context we may recall the instructive discussion given by Sedighi and Palasantzas [31]: they replaced the upper plate by a metal sphere (gold) with mass M and radius R, elastically suspended in the gravitational field and able to move vertically with velocity $\dot{z}$ under the combined influence of gravity, viscous drag from the environment (in their case air), and Casimir force from the plate beneath. The key difference from our case is that we consider a liquid-induced drag instead of an air-induced one. One can set up the governing equation and from that estimate the viscous decay time. We have gone through this calculation under our conditions, assuming a gold sphere with $R = 10\,\mu\text{m}$, sphere velocity $\dot{z} = 3\,\text{mm/s}$ typically, and viscosity being the same as for water. Under these conditions, the Reynolds number is very small; hence, the Stokes drag formula is applicable. We omit the details here, but the result is that the decay time becomes small, of the order of milliseconds. This result is promising as the decay time is much smaller than the time scale needed for the full tin phase transition and the actuator can, in our case, be considered to be reacting instantaneously. We point out that such devices are not limited to the particular materials chosen nor the type of metal/nonmetal transition. Other combinations of materials and phase transitions can be chosen, tailored to the second surface in order to control switching and phase-transition time.

VII. CONCLUSIONS

In conclusion, we have shown that by exploiting the combined effect of (i) the tin phase transition and (ii) fluid-mixture composition, it becomes possible to fabricate a switch operative at a moderate temperature range. A repulsive interaction is found in semimetallic α-Sn when the chlorobenzene content is mixed with bromobenzene (the specific critical concentration depends on the type of silica). The repulsive interaction switches to attraction when there is as little as 6% conversion of α-Sn to β-Sn. It also switches when the chlorobenzene content rises above the critical concentration. We have verified that our model accurately can represent a 0.1-μm-thick SiO_2 slab with a 1-μm^2 contact area and that the buoyancy pressure and thermal effects then are negligible. For distances around 20 Å between Sn and SiO_2 surfaces, the repulsive Lifshitz free energy exceeds $600 k_B T$ for α-Sn, and its energy barrier is sufficiently large relative to the thermal energy, indicating that the attractive interaction for β-Sn is stable. Hence, thermodynamically stable nanoswitching can be achieved. We think that the idea is worth noticing for its possible applications in nanomechanical systems and environmental sensors.

ACKNOWLEDGMENTS

We acknowledge financial support from the Research Council of Norway (Projects No. 221469 and No. 250346) and access to high-performance computing resources via SNIC and NOTUR.

---

[1] H. B. G. Casimir, Proc. K. Ned. Akad. Wet. **51**, 793 (1948).

[2] I. E. Dzyaloshinskii, E. M. Lifshitz, and L. P. Pitaevskii, Sov. Phys. Usp. **4**, 153 (1961).

[3] F. M. Serry, D. Walliser, and G. J. Maclay, J. Appl. Phys. **84**, 2501 (1998).

[4] B. Bhushan, J. Vac. Sci. Technol. B **21**, 2262 (2003).

[5] B. W. Ninham and V. A. Parsegian, Biophys. J. **10**, 646 (1970).

[6] C. H. Anderson and E. S. Sabisky, Phys. Rev. Lett. **24**, 1049 (1970).

[7] F. Hauxwell and R. H. Ottewill, J. Colloid Interface Sci. **34**, 473 (1970).

[8] P. Richmond and B. W. Ninham, J. Low Temp. Phys. **5**, 177 (1971).

[9] P. Richmond, B. W. Ninham, and R. H. Ottewill, J. Colloid Interface Sci. **45**, 69 (1973).

[10] S. K. Lamoreaux, Nature (London) **457**, 156 (2009).

[11] P. J. van Zwol and G. Palasantzas, Phys. Rev. A **81**, 062502 (2010).

[12] M. Boström, B. E. Sernelius, I. Brevik, and B. W. Ninham, Phys. Rev. A **85**, 010701 (2012).

[13] V. Esteso, S. Carretero-Palacios, and H. Miguez, J. Phys. Chem. C **119**, 5663 (2015).

[14] A. Milling, P. Mulvaney, and I. Larson, J. Colloid Interface Sci. **180**, 460 (1996).

[15] S.-w. Lee and W. M. Sigmund, J. Colloid Interface Sci. **243**, 365 (2001).

[16] A. A. Feiler, L. Bergström, and M. W. Rutland, Langmuir **24**, 2274 (2008).

[17] J. N. Munday, F. Capasso, and V. A. Parsegian, Nature (London) **457**, 170 (2009).

[18] G. Bimonte, E. Calloni, G. Esposito, L. Milano, and L. Rosa, Phys. Rev. Lett. **94**, 180402 (2005).

[19] F. Chen, G. L. Klimchitskaya, V. M. Mostepanenko, and U. Mohideen, Opt. Express **15**, 4823 (2007).

[20] G. Bimonte, E. Calloni, G. Esposito, and L. Rosa, Nucl. Phys. B **726**, 441 (2005).

[21] G. L. Klimchitskaya, U. Mohideen, and V. M. Mostepanenko, J. Phys. A **40**, F841 (2007).

[22] R. Castillo-Garza, C.-C. Chang, D. Jimenez, G. L. Klimchitskaya, V. M. Mostepanenko, and U. Mohideen, Phys. Rev. A **75**, 062114 (2007).

[23] G. Bimonte, Phys. Rev. A **78**, 062101 (2008).

[24] A. Benassi and C. Calandra, Europhys. Lett. **84**, 11002 (2008).

[25] I. Pirozhenko and A. Lambrecht, Phys. Rev. A **77**, 013811 (2008).

[26] R. Esquivel-Sirvent, Phys. Rev. A **77**, 042107 (2008).

[27] E. G. Galkina, B. A. Ivanov, S. Savel'ev, V. A. Yampol'skii, and F. Nori, Phys. Rev. B **80**, 125119 (2009).

[28] G. Torricelli, P. J. van Zwol, O. Shpak, C. Binns, G. Palasantzas, B. J. Kooi, V. B. Svetovoy, and M. Wuttig, Phys. Rev. A **82**, 010101(R) (2010).

[29] G. Torricelli, P. J. van Zwol, O. Shpak, G. Palasantzas, V. B. Svetovoy, C. Binns, B. J. Kooi, P. Jost, and M. Wuttig, Adv. Funct. Mater. **22**, 3729 (2012).

[30] M. Sedighi, W. H. Broer, G. Palasantzas, and B. J. Kooi, Phys. Rev. B **88**, 165423 (2013).

[31] M. Sedighi and G. Palasantzas, Appl. Phys. Lett. **104**, 074108 (2014).

[32] M. Sedighi and G. Palasantzas, J. Appl. Phys. **117**, 144901 (2015).

[33] L. Viña, H. Höchst, and M. Cardona, Phys. Rev. B **31**, 958 (1985).

[34] M. Iizumi, Phys. B (Amstedam, Neth.) **136**, 36 (1986).

[35] Ch. Wohlfarth, *Static Dielectric Constants of Pure Liquids and Binary Liquid Mixtures*, edited by O. Modelung, Landolt-Börnstein, Group IV, New Series Vol. 6 (Springer, Berlin, 1991).

[36] D. E. Aspnes, Am. J. Phys. **50**, 704 (1982).

[37] P. Blaha, K. Schwarz, G. K. H. Madsen, D. Kvasnicka, and J. Luitz, WIEN2k, An Augmented Plane Wave + Local Orbitals Program for Calculating Crystal Properties (Karlheinz Schwarz, Technische Universität Wien, Austria, 2001).

[38] C. Ambrosch-Draxl and J. O. Sofo, Comput. Phys. Commun. **175**, 1 (2006).

[39] *Group IV Elements, IV-IV and III-V Compounds, Part b - Electronic, Transport, Optical and Other Properties*, edited by O. Madelung, U. Rössler, and M. Schulz, Landolt-Börnstein - Group III Condensed Matter, Vol. 41A1ß (Springer, Berlin, 2002).

[40] C. Persson and S. Mirbt, Braz. J. Phys. **36**, 286 (2006).

[41] A. Crovetto, R. Chen, R. B. Ettlinger, A. C. Cazzaniga, J. Schou, C. Persson, and O. Hansen, Sol. Energy Mater. Sol. Cells **154**, 121 (2016).

[42] V. A. Parsegian and B. W. Ninham, Biophys. J. **10**, 664 (1970).

[43] J. N. Israelachvili, *Intermolecular and Surface Forces*, 3rd ed. (Academic, Waltham, MA, 2011).

[44] M. Boström, O. I. Malyi, P. Parashar, K. V. Shajesh, P. Thiyam, K. A. Milton, C. Persson, D. F. Parsons, and I. Brevik, Phys. Rev. B **95**, 155422 (2017).

[45] M. Boström, O. I. Malyi, P. Thiyam, K. Berland, I. Brevik, C. Persson, and D. F. Parsons, Europhys. Lett. **115**, 13001 (2016).

[46] O. I. Malyi, M. Boström, V. V. Kulish, P. Thiyam, D. F. Parsons, and C. Persson, Phys. Chem. Chem. Phys. **18**, 7483 (2016).

[47] I. Brevik, S. A. Ellingsen, and K. A. Milton, New J. Phys. **8**, 236 (2006).

[48] A. T. Poortinga, R. Bos, and H. J. Busscher, Langmuir **17**, 2851 (2001).

[49] D. Grasso, K. Subramaniam, M. Butkus, K. Strevett, and J. Bergendahl, Rev. Environ. Sci. Biotechnol. **1**, 17 (2002).

[50] Y.-I. Chang and P.-K. Chang, Colloids Surf. A **211**, 67 (2002).

[51] K. Nogita, C. M. Gourlay, S. D. McDonald, S. Suenaga, J. Read, G. Zeng, and Q. F. Gu, Philos. Mag. **93**, 3627 (2013).